Numerical and Analytical Estimates of M_2 Tidal Conversion at Steep Oceanic Ridges

EMANUELE DI LORENZO

School of Earth and Atmospheric Sciences, Georgia Institute of Technology, Atlanta, Georgia

WILLIAM R. YOUNG

Scripps Institution of Oceanography, University of California, San Diego, La Jolla, California

STEFAN LLEWELLYN SMITH

Department of Mechanical and Aerospace Engineering, University of California, San Diego, La Jolla, California

(Manuscript received 26 April 2004, in final form 8 April 2005)

ABSTRACT

Numerical calculations of the rate at which energy is converted from the external to internal tides at steep oceanic ridges are compared with estimates from analytic theories. The numerical calculations are performed using a hydrostatic primitive equation ocean model that uses a generalized *s*-coordinate system as the vertical coordinate. The model [Regional Ocean Modeling System (ROMS)] estimates of conversion compare well with inviscid and nondiffusive theory in the sub- and supercritical regimes and are insensitive to the strength of viscosity and diffusivity. In the supercritical regime, the nondissipative analytic solution is singular all along the internal tide beams. Because of dissipation the ROMS solutions are nonsingular, although the density gradients are strongly enhanced along the beams. The agreement between model and theory indicates that the prominent singularities in the inviscid solution do not compromise the estimates of tidal conversion and that the linearization used in deriving the analytical estimates is valid. As the model beams radiate from the generation site the density gradients are further reduced and up to 20% of the energy is lost by model dissipation (vertical viscosity and diffusion) within 200 km of the ridge. As a result of the analysis of the numerical calculations the authors also report on the sensitivity of tidal conversion to topographic misrepresentation errors. These errors are associated with inadequate resolution of the topographic features and with the smoothing required to run the ocean model. In regions of steep topographic slope (i.e., the Hawaiian Ridge) these errors, if not properly accounted for, may lead to an underestimate of the true conversion rate up to 50%.

1. Introduction

Ocean tides are an important source of mechanical energy required to mix the global ocean (Garrett and St. Laurent 2002). Tidal forces perform about 3.5 TW of work, of which 2.5 TW is contributed by the semidiurnal tide alone (Munk and Wunsch 1998). Recent studies using satellite altimetry and ocean models show that most of the energy conversion from the external to internal tides occurs over island chains, oceanic trenches, and midocean ridges. Examples include the Hawaiian Ridge, the Izu Ridge, and the Mendocino Escarpment (Althaus et al. 2003; Cummins et al. 2001; Egbert and Ray 2000, 2001; Kang et al. 2000; Merrifield and Holloway 2002; Niwa and Hibiya 2001). However, there are significant uncertainties in these estimates of energy conversion.

For example, over the Hawaiian Ridge, Egbert and Ray (2000) estimate a total of 20 GW of energy loss from the barotropic tide. The energy dissipated by bottom friction is small (Garrett and St. Laurent 2002) so that most of this energy must be transferred into the internal tides. However, model estimates of conversion and the resulting energy flux carried by internal tides disagree by up to 50%. Niwa and Hibiya (2001) use an *s*-coordinate three-dimensional ocean model and obtain 15 GW of barotropic energy conversion over the Hawaiian Ridge by the M_2 tide [to compare with the 20 GW estimated by Egbert and Ray (2000)]. Merrifield

Corresponding author address: Emanuele Di Lorenzo, School of Earth and Atmospheric Sciences, Georgia Institute of Technology, 311 Ferst Drive, Atlanta, GA 30332-0340.
E-mail: edl@eas.gatech.edu

and Holloway (2002) use the same type of model and account for about 10 GW of radiated energy away from the ridge (with a 10% uncertainty in the estimate). In their study Merrifield and Holloway do not report an estimate of the model conversion at the ridge and argue that the remaining unaccounted 10 GW may be dissipated locally by other means (e.g., turbulent mixing). However, they are unable to verify this effect in the model run.

There are several explanations for differences among model results. These include different parameterizations of unresolved physical processes, such as mixed layer dynamics, bottom boundary layer schemes, and small-scale instabilities. Because the conversion rate is very sensitive to bottom topography and stratification, the different density fields and topographies used in the simulations may also play an important role.

Theoretical estimates of tidal conversion are a complementary approach to the problem of tidal conversion by a very steep ridge, but theoretical estimates are beset by their own uncertainties, which differ from those of models. It is our goal here to make a comparison between model and theoretical estimates of tidal conversion at a steep ridge and in doing so develop confidence in both approaches. Khatiwala (2003) has taken a similar approach to understanding tidal conversion by a "truncated sinusoidal bathymetry." However, the theoretical estimates in that work are based on the weak topography approximation of Bell (1975). Recent theoretical developments allow us to proceed beyond this simple approximation and consider realistically steep and tall bathymetry.

St. Laurent et al. (2003) proposed the "knife-edge barrier" as a theoretical idealization of a very steep ridge. Using a numerical method St. Laurent et al. (2003) then computed the radiated power from this obstacle and other abrupt topographies. Llewellyn Smith and Young (2002) subsequently found an analytic solution for the power radiated by a knife-edge barrier.

Idealizing a ridge of finite width by the zero-width knife edge might seem implausible. However, using a combination of numerical and analytic methods Pétrélis et al. (2006) computed the power radiated by two different ridge profiles (a triangle and a polynomial; see section 2) in which the width is a parameter. By varying the width it is possible to pass continuously from the knife-edge limit of St. Laurent et al. (2003) to the complementary case of a gently sloping ridge. A main conclusion of Pétrélis et al. (2006) is that the super- to subcritical transition is continuous and that the knife-edge model is indicative of both conversion rates and the structure of the radiated wave field over much of the supercritical parameter range.

The results of St. Laurent et al. (2003), Llewellyn Smith and Young (2002, 2003), and Pétrélis et al. (2006) are all obtained by ignoring diffusion, viscosity, and nonlinearity. With this neglect, the solutions in the supercritical regime are singular all along the tidal beams. Robinson (1969), who analyzed the structure of this singularity in a related example, referred to the tidal beam as a "singular characteristic," and showed that the narrow region surrounding the beam does not act as a source of mass, momentum, or energy for the remainder of the flow. Thus, the singularity is milder than other well-known hydrodynamic singularities (e.g., hydraulic jumps act as sinks of energy). Balmforth et al. (2002) show how the singularity is approached as the amplitude of subcritical sinusoidal topography is increased until the critical condition (i.e., ray slope equals topographic slope) is achieved. Thus, even subcritical solutions exhibit an attenuated form of the singularity if the ray slope is only slightly greater than the topographic slope. This singularity of the linear and inviscid solution indicates missing physics and leads one to wonder if the resulting theoretical estimates of tidal conversion are compromised.

Polzin (2004) argues that there is an additional problem with the linear estimates of tidal conversion summarized above. Polzin notes that in addition to simplification of the bottom boundary condition these calculations also neglect certain *linear* terms, namely, the advection of perturbation velocity by the barotropic tidal flow. This approximation is justified by scale analysis, provided that the tidal excursion distance (typically 100 or 200 m) is much less than the length scale of the topography. However, neglect of the tidal momentum advection is not a necessary approximation: using a Lagrangian approach Bell (1975) retains these tidal advection terms, and this is a chief source of algebraic complexity in Bell's work. Comparison with Bell's results confirms that the neglect of tidal advection is indeed justified for topography whose scale is greater than the tidal excursion distance. Polzin's main point is that there is significant topographic roughness on a scale of 100 or 200 m. On these small scales, neglect of the tidal advection produces a large overestimate of *shear* in the wave field radiated from small-scale topography. Moreover, even without small-scale topography, linear generation theories predict infinite shear in the supercritical regime: for example, the solutions of Balmforth et al. (2002) show how small-scale features develop in the wave field as a single large-scale topographic sinusoid approaches critical slope. The development of small scales, and infinite shear, is evident also from Robinson's (1969) analysis of the velocity close to the tidal beam: Robinson shows that, as the

singular beam is approached, the tangential velocity to the beam becomes infinite with an algebraic singularity, while the normal velocity is continuous. The tangential shear, which is the normal derivative of the tangential velocity, is strongly singular. Thus, we agree with Polzin (2004) that *shear* cannot be reliably predicted by recent linear solutions. Nonetheless, we argue that this problem with shear does not compromise the rest of the solution and that the estimates of radiated *energy* are reliable. A main goal of this paper is to support this view with a successful comparison between linear theory and a numerical model. The point is that the linear solutions all indicate that the radiated energy is heavily concentrated in the first two or three vertical modes: both the model and the theory are reliable for these large-scale motions.

In the next sections we present tidal conversion estimates over ridges with different shapes, obtained using a hydrostatic primitive equation ocean model that uses a generalized *s*-coordinate system as the vertical coordinate. These model estimates compare well with inviscid and nondiffusive theory in the sub- and supercritical regimes. The agreement between model and theory indicates that the prominent singularities in the inviscid analytical solution do not compromise the estimates of tidal conversion and that the linearization used in deriving the analytical estimates is valid. We also present evidence that topographic misrepresentation errors associated with inadequate resolution of the topographic features and with the smoothing required to run the ocean model can lead to underestimation of the true conversion rate up to 50%.

2. The model

The model used in this study is a hydrostatic *s*-coordinate code: the Regional Ocean Modeling System (ROMS; Haidvogel et al. 2000). ROMS solves the primitive equations on a curvilinear horizontal grid and on a generalized *s*-coordinate system in the vertical. The model uses the Boussinesq and hydrostatic approximations. A detailed description of the model numerics can also be found in Shchepetkin and McWilliams (1998, 2003).

a. Basic configuration

The "basic configuration" is a rectangular basin of dimensions 1200 km × 100 km (x, y). The grid resolution is 1.5 km in the horizontal plane. In the vertical direction, 40 levels are equally spaced to cover the total depth of the ocean ($H = 2000$ m). In the basic configuration, the model does not employ explicit horizontal dissipation. In the vertical direction there is viscosity and diffusivity, both equal to 10^{-5} m^2 s^{-1}; there is no explicit mixed layer scheme. At the bottom a free-slip condition is used with no bottom drag in order to isolate the energy conversion from a barotropic to baroclinic tide. The conversion estimates are computed over a "polynomial" ridge:

$$h = h_{\max}\begin{cases}\left(1 - \dfrac{x^2}{a^2}\right)^2 & \text{if } |x| < a \\ 0 & \text{if } |x| > a\end{cases},$$

with $a = 10$ and 30 km. The height of the bump $h_{\max}$ is an input parameter of the model. Notice that h and dh/dx are continuous at $x = \pm a$. The horizontal/vertical resolution of the model is adequate to resolve these ridge shapes; however, we also explored the effects of topographic misrepresentation errors associated with changes in the horizontal and vertical resolution, and with smoothing (section 4). For all model calculation we use a linear equation of state.

b. Initial and boundary conditions

The model is initialized with constant stratification set by a uniform buoyancy frequency, N, which is set as a model input parameter. The M_2 tide is forced by adding a body force in the horizontal momentum equations, $B_u(t) = \omega U_o \cos(\omega t)$ and $B_v(t) = fU_o \sin(\omega t)$. With a flat bottom the resulting external tidal velocity in the x direction is then $U = U_o \sin(\omega t)$ and $V = 0$, where $\omega = 2\pi/(12.4\text{ h})$ is the frequency of the M_2 tide. We take $U_o = 2$ cm s^{-1}. We concluded that in the x direction the cleanest approach is to use periodic boundary conditions instead of radiation conditions (section 4 discusses some of the technical issues related to the ill-posed boundary conditions).

With this setup the domain is closed and finite and there is no issue with open boundaries and radiation conditions. There is then no need to design a "sponge layer." However, the time span of the integration must be limited so that the domain does not "fill up" with energy. In other words, we must estimate the conversion before the radiation has time to travel around the reentrant domain and interfere with the generation process at the ridge.

In the basic configuration the domain length in x is 1200 km. During the 12 tidal cycles (n_{cycle}) of the model integration a vertical mode 1, with M_2 tidal frequency, will propagate approximately $\Delta x \simeq 500$ km given a buoyancy frequency of $N = 2 \times 10^{-3}$ s^{-1} (the maximum value used in the simulations). Specifically,

$$\Delta x = \frac{Hn_{\text{cycle}}}{\alpha},$$

where $H = 2000$ m is the depth of the ocean and α is the slope of the internal beams given by

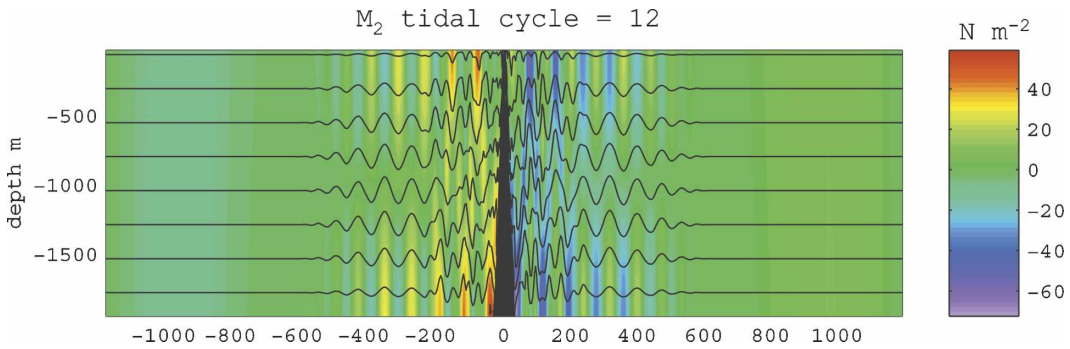

FIG. 1. Vertical sections of perturbation pressure (N m^{-2}) after 12 tidal cycles with h_{max} = 1600 m and $N = 2 \times 10^{-3}$ s^{-1}. The isopycnal displacements (black lines) are increased in magnitude by a factor of 10 to show the internal tides. The model has periodic open boundary condition and is driven by a tidal body force.

$$\alpha = \left(\frac{\omega^2 - f^2}{N^2 - \omega^2}\right)^{1/2}.$$

For the Coriolis parameter $f = 10^{-4}$ s^{-1} and the M_2 tidal frequency ω is

$$\alpha = 0.1 \quad \text{for} \quad N = 1 \times 10^{-3} \quad \text{and}$$

$$\alpha = 0.05 \quad \text{for} \quad N = 2 \times 10^{-3}.$$

Figure 1 shows a model simulation with double the domain size in the x direction (i.e., 2400 km) to clearly show the extent of the internal tide propagation after 12 tidal periods. The model estimates of tidal conversion obtained from the solution in Fig. 1 are exactly the same as those obtained using the smaller 1200 km domain in the basic configuration. On the contrary, if we make the domain very short in the x direction, for example 150 km, the internal beams are allowed to propagate back in the domain and the tidal energy conversion saturates quickly, leading to a zero energy flux.

c. Diagnosing the conversion rate

To compare the numerical model tidal conversion rate with theory we define the conversion rate in the model as the sum of the baroclinic wave energy flux radiated through sections to the west and east of the ridge, located where the height of the ridge goes to zero ($\pm a$):

$$C_{\text{model}} = Ef(a) - Ef(-a) = 2Ef(a),$$

where the time, depth, and along-ridge average energy flux Ef at location x is defined as

$$Ef(x) = \rho_0 \frac{\omega}{8\pi} \int_{2\pi n/\omega}^{2\pi(n+4)/\omega} \frac{1}{h(x)L_y} \int_{-h}^{\eta} \int_{-L_y/2}^{L_y/2} p'(x, y, z, t)u'(x, y, z, t)\, dy\, dz\, dt, \quad (1)$$

where $\rho_0 = 1025$ is the reference density, p' and u' are the perturbation pressure and velocity, $\eta(x, y, t)$ is the model free surface, L_y is the along-ridge extent of the model domain, and h is the absolute depth of the ocean. The model is spun up for three tidal cycles, and the time integral is evaluated over tidal cycles 4–8 ($n = 4$) and 8–12. We define perturbation quantities as the deviation from the barotropic as follows:

$$p'(x,y,z,t) = \rho_0 g(\eta - \eta_B) + p(x,y,z,t) - p_0(z) \quad \text{and}$$

$$u'(x,y,z,t) = u(x,y,z,t) - \frac{1}{h}\int_{-h}^{\eta} u(x, y, z, t)\, dz\,,$$

where the subscript B denotes the barotropic component of the free surface; p is the total pressure field, not including the free-surface contribution, and $p_0(z)$ the pressure field of the fluid at rest. To accurately compute and separate the barotropic component of the free surface, Khatiwala (2003) separates the free-surface response of the external tide from the internal tide by preceding each model integration with a barotropic model run (i.e., no stratification). However, in our computation of the energy flux [Eq. (1)] we do not need to compute the term $\rho_0 g(\eta - \eta_B)$ in the perturbation pressure. This term does not have a vertical dependence and it vanishes when dotted with u' and integrated in the vertical. By definition, u' has zero vertical integral. In Khatiwala this term is retained because the actual conversion is estimated using the perturbation pressure at the bottom over the topography.

In this regard it is important to note a potential flaw with the definition of p'. The barotropic tidal solution will be slightly different for the unstratified and stratified simulations. This is because the internal tide acts as a drag mechanism on the barotropic tide. Thus, the barotropic currents will be weaker in the stratified run

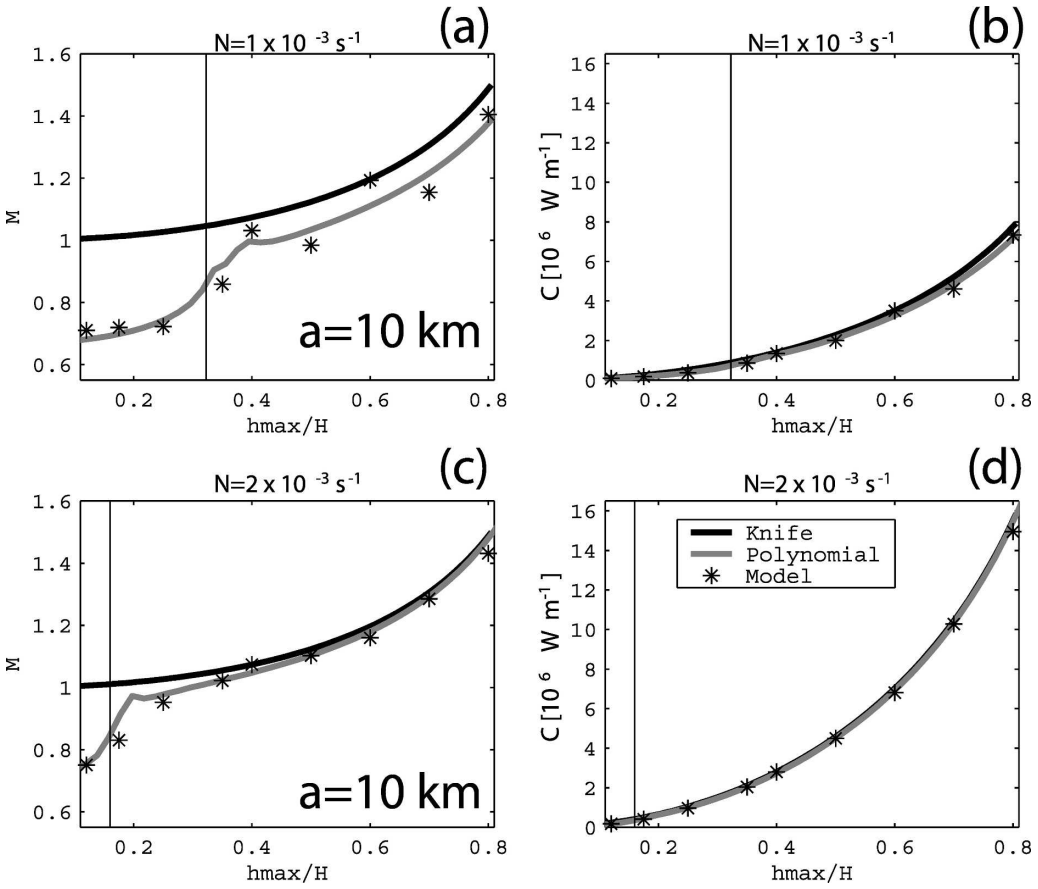

FIG. 2. Model estimates of M for polynomial ridge (a= 10 km) with stratification (a), (b) $N = 1 \times 10^{-3}$ s^{-1} and (c), (d) N $= 2 \times 10^{-3}$ s^{-1}. The tidal conversion per unit ridge in the alongshore direction (L_y = 100 km) is reported in (b) and (d), and C is given in section 2c. The gray solid line is the analytical prediction from the Pétrélis et al. (2006) theory, and the black line is from the knife-edge mode (St. Laurent et al. 2003). The black vertical lines in each panel represent the transition from subcritical to supercritical regime, and H = 2000 m in the model simulations.

and introduce a source of error in p' associated with the term $\rho_0 g(\eta - \eta_B)$.

3. Comparison of theory and model

Pétrélis et al. (2006) provide a unified analytical expression for the conversion rate of a ridge that holds for sub- and supercritical conditions as well as the transition regime. The conversion rate is expressed as

$$C = \frac{1}{4}\pi\rho_0 U_0^2 N h_{\max}^2 \sqrt{1 - (f/\omega)^2} \times M\left(\frac{\alpha a}{H}, \frac{h_{\max}}{H}\right), \tag{2}$$

where M is a dimensionless function that depends on parameters $\alpha a/H$ and $h_{\max}/H$. We use the procedure of Pétrélis et al. (2006), based on solving an integral equation, to obtain M. The dimensional factor on the right-hand side of Eq. (2) has units of watts per unit meter of along-ridge extent in the y direction. This factor contains the strongest dependence of C on the external parameters. The square-root term and M are both weakly varying functions over the parameter range that we explore.

We performed model simulations for the polynomial ridge with different stratifications $N = 1 \times 10^{-3}$ and 2×10^{-3} s^{-1} and for two different ridge widths, a = 10 km and a = 30 km. For each regime we also investigate different values of $h_{\max}/H$ by varying the height of the bump. The model estimates are reported in Figs. 2 and 3, both as total conversion rate (W m^{-1}) and using the dimensionless function M, defined in Eq. (2). The dimensional representation on the left (W m^{-1}) is very forgiving of small differences between model and analytics: the results agree to within line widths over large variations in the parameter $h_{\max}/H$. Expressing the re-

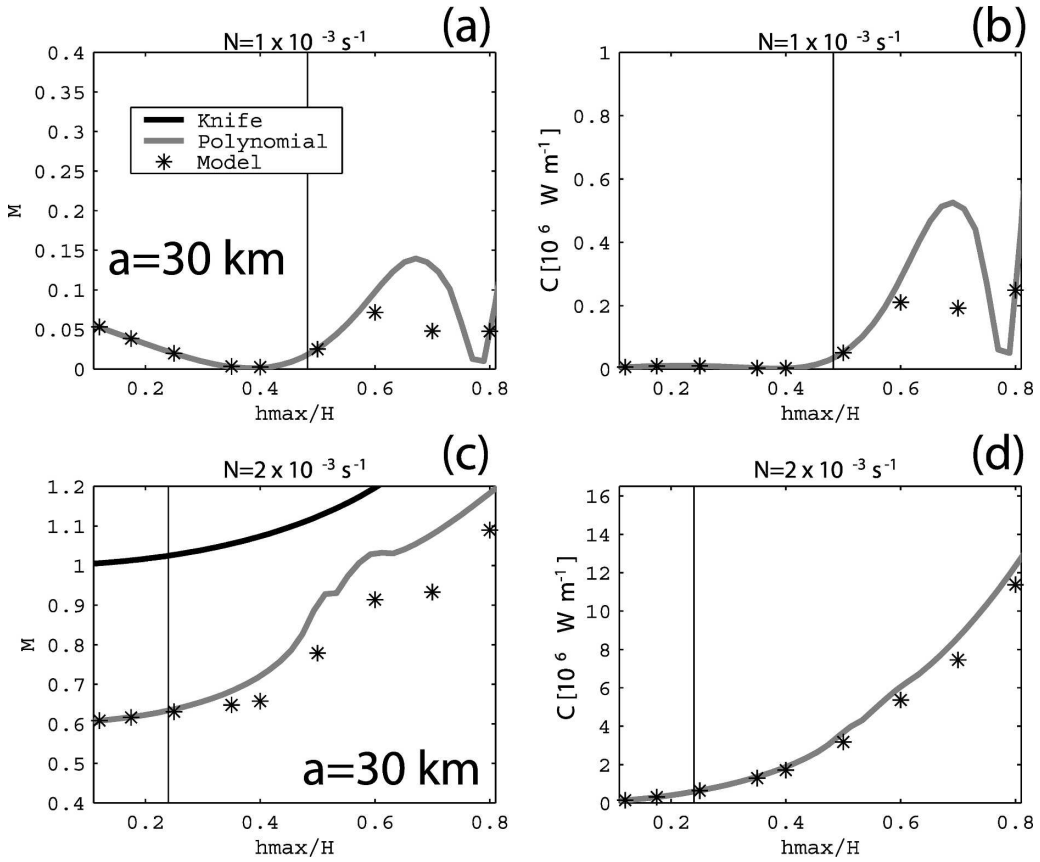

FIG. 3. Model estimates of M for polynomial ridge (a = 30 km) with stratification (a), (b) $N = 1 \times 10^{-3}$ s^{-1} and (c), (d) N = 2×10^{-3} s^{-1}. The tidal conversion per unit ridge in the alongshore direction (L_y = 100 km) is reported in (b) and (d), and C is given in Eq. (1). The gray solid line is the analytical prediction from the Pétrélis et al. (2006) theory, and the black line is from the knife-edge mode (St. Laurent et al. 2003). The black vertical lines in each panel represent the transition from subcritical to supercritical regime, and H = 2000 m in the model simulations.

sults in terms of M (the right-hand panels in Fig. 2 and Fig. 3) emphasizes the differences between the model and theory. We regard the comparison as satisfactory. The model estimates are smaller than the theoretical estimates, typically by about –2.5% with standard deviation of 3.5%. This underestimate may be associated with the nonzero dissipation in the model (in contrast with the inviscid theory prediction) and with inadequate representation of the topography by the model's s-coordinate system for the polynomial ridge. The exact algebraic expression for the polynomial ridge goes to zero sharply at $x = \pm a$. The s coordinate is a terrain-following coordinate system and enforces smooth transitions from one grid point to the other so that ROMS can only approximate the discontinuous second derivatives at $x = \pm a$ of the polynomial ridge. The resulting smoothing of the ridge always leads to a smaller conversion rate [e.g., see Fig. 1 in Pétrélis et al. (2006), which shows about a 5% reduction in M from the triangular ridge to a comparable smooth ridge]. More detail is provided in section 4 on this type of topography misrepresentation error.

Because the model estimates are obtained using the full nonlinear model, the relatively good comparison with theory suggests that the linear assumption used in the analytic studies is valid. We also performed model calculations in which we drop the nonlinear terms in the momentum equations while retaining them for the bouyancy (we refer to these calculations as "linear model," as opposed to "nonlinear model," which retains all the terms in the equation). The conversion rate estimates are not significantly different.

However, as the waves radiate away from the ridge, the rate at which the energy is lost to dissipation is different for the linear and nonlinear case. By evaluating the wave energy flux across different vertical sections away from the ridge we can estimate how much of the initial wave internal energy is dissipated as a func-

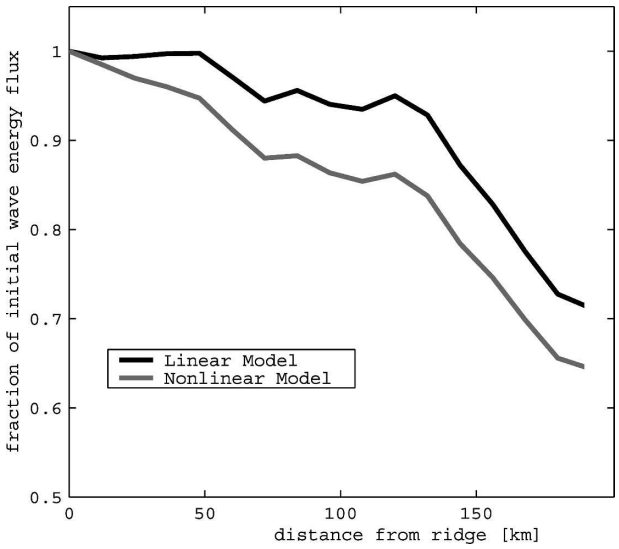

FIG. 4. Energy flux as a function of distance from the ridge. The energy flux has been rescaled by the energy flux adjacent to the ridge. The curves are obtained by averaging all the experiments for the polynomial ridges with different heights and stratifications. The nonlinear case is the basic configuration (gray line). Experiments that do not retain advection in the momentum equation are referred as linear (black line).

tion of the distance from the ridge (Fig. 4). For the linear case 20% of the energy flux is lost within 200 km from the ridge. (To estimate correctly the flux beyond 200 km we would need longer model integrations.) In the nonlinear case, although the initial energy flux is not significantly different from the linear case, the attenuation is more rapid within the first 50 km. After 200 km of radiation from the ridge 30% of the initial energy flux is lost. These estimates are insensitive to vertical diffusivity and viscosity: increasing the coefficient from 10^{-5} to 10^{-4} or even 10^{-3} m^2 s^{-1} makes no difference (significant differences start occurring for 10^{-1} m^2 s^{-1}). This is expected from dimensional analysis: with a diffusivity of 10^{-3} m^2 s^{-1} it would take approximately 28 days to diffuse density or momentum over the vertical length scale of a model grid box (50 m). This time scale is longer than the duration of the integrations (6 days). Therefore, the decay of the radiated energy flux must be associated to nonlinear interactions and to the implicit numerical dissipation such as the time-stepping scheme, the filter used to average the barotropic fast time-stepping, and the advection scheme. Future studies that aim to correctly quantify the dissipation rate of the radiated flux as a function of distance from the generation site will need to assess the sensitivity to these factors more rigorously. However, these effects are unimportant in estimating the conversion and energy fluxes over, and in proximity (50 km) of, the ridge.

4. Numerical aspects

In this section we provide additional details about the numerical setup for the open boundary conditions and a discussion of the errors associated with misrepresentation of the topography. The goal is to provide sufficient information to enable an independent reproduction of the numerical estimates presented in the section above.

a. Radiation condition plus tidal forcing at the open boundary

A common approach used in *s*-coordinate models to simulate tidal conversion over oceanic ridges such as the Hawaiian Ridge is to use a radiation condition for the baroclinic variables and to prescribe the M_2 tidal velocities and elevations at the open boundary through a forced-gravity-wave radiation condition in the barotropic variables (Niwa and Hibiya 2001; Merrifield and Holloway 2002).

As an alternative to the periodic boundary conditions used in the "basic configuration" we also performed calculations using this type of boundary condition for the barotropic variables combined with an existing implicit radiation boundary condition for the baroclinic variables implemented in ROMS by Marchesiello et al. (2003).

We find that also with this configuration the model M_2 barotropic velocity is accurately reproduced, and the conversion estimate leads to the same results as in the periodic settings. Some spurious effects in proximity of the open boundary were observed but apparently did not significantly affect our estimate of the radiated energy flux.

b. Radiation condition plus body force

We also performed computation using the approach of Khatiwala (2003), who combined radiation conditions for the model variables with a body force, as the one mentioned above for the periodic boundary case. In ROMS, this approach was able to generate the appropriate tidal velocity in the interior only during the first tidal cycle. In subsequent tidal cycles the magnitude of the velocity is reduced and the oscillatory behavior of the tidal forcing disappears. We decided not to investigate further this approach.

c. Cautionary remarks on the effects of topography misrepresentation

A common practice in the use of a terrain-following coordinate system is to smooth the topographic gradients to minimize the numerical errors associated with

the computation of the pressure gradient term (Mellor et al. 1994). Although all of the calculations presented in the previous sections had enough resolution so that no smoothing was required, more realistic calculations often cannot avoid it. The criterion used to define the amount of smoothing is to reduce the r factor, which is an indicator of the topographic slope relative to the model grid:

$$r = \left| \frac{h_{i-1} - h_i}{h_{i-1} + h_i} \right|,$$

where h is the topography and the indices i indicate a model grid point. A discussion of the r factor is provided in Haidvogel and Beckmann (1999). However, there is no study that documents an objective method to choose the appropriate r. Based on experience, modelers smooth the bathymetry in order to keep the $r < 0.2$. Because the filters used for smoothing topography will result in a reduction of the ratios $h_{\max}/a$ and $h_{\max}/H$, this implies that global estimates of conversion done with s-coordinate models will always lead to an underestimate of the tidal conversion. The question is how much.

Figure 5 shows a comparison of the shapes of the ridge for different grid resolutions (0.8, 1.5, 2.5, and 4 km) before and after the smoothing. After the smoothing the r factor is reduced to 0.2 for both cases (we used a Shapiro filter for the smoothing). In the cases $dx = 0.8$ km and $dx = 1.5$ km no smoothing is necessary as the r factor is already below 0.2. Instead, for $dx = 2.5$ km and $dx = 4$ km the initial r factor is 0.29 and 0.43, respectively. The resulting smoothed version of the ridge is shown as the dashed line in the bottom panels of Fig. 5. If we define the error percent in the tidal conversion estimate as a deviation from the analytical prediction,

$$\text{error} = \frac{C_{\text{model}} - C_{\text{theory}}}{C_{\text{theory}}} \times 100,$$

we find that, after the smoothing, the tidal conversion was reduced in cases $dx = 2.5$ km and $dx = 4$ km by 12% and 17%, respectively. By performing this same analysis using different initial values $h_{\max}/a$ and different buoyancy frequency ranging from 0.001 to 0.01 s^{-1} we find that on average there is a 20% reduction in conversion rate for a change in the r factor of 0.1. The results of this analysis are shown in Fig. 6a where the percentage reduction of conversion rate is plotted against the dr change that occurred after the smoothing. Reducing the r factor by smoothing may inadvertently reduce $h_{\max}$. For simple analytical examples, such as the polynomial ridge, this effect on the conversion rate is obvious and can be quantified. However, for more complicated topographies quantifying the reduction of the conversion rate is not straightforward. For the model cases with resolution ≤ 1.5 km the r factor is always < 0.2, so there is no need to apply smoothing and the estimates converge to the same value.

This is one example of topography misrepresentation error. Alternatively one could decide not to apply any smoothing. We therefore perform all of the model simulations leaving the r factor unchanged and plot the errors in the estimate as a function of the maximum r factor (Fig. 6b). The figure shows marks with large errors, but they do not appear to have a linear relationship with r. Further analysis reveals that a better criterion to distinguish the model error estimates is associated with how well the ridge is resolved by the model grid size (horizontal resolution). We define this misrepresentation error as the percentage volume of the ridge not accounted for by the model coordinate system:

$$\text{resolution error} = \frac{|\text{ridgeV}_{\text{model}} - \text{ridgeV}_{\text{analytical}}|}{\text{ridgeV}_{\text{analytical}}} \times 100.$$

In Fig. 6b most of the model simulations with resolution error higher than 1% and 5% overestimate the tidal conversion predicted from theory (by 15% and 35% on average). This is expected because, if we decrease the resolution without applying any smoothing, the effective shape of the ridge becomes rougher (i.e., looks more like a staircase: Fig. 5d, thick black line).

The range of uncertainties that arise from model calculation that use a smooth versus nonsmooth representation of the topography, in cases for which the grid resolutions cannot fully resolve (within 1%) the shape of the ridge, could play a major role in explaining some of the discrepancies in global numerical estimates of tidal conversion.

5. Summary, conclusions, and discussion

We compare and discuss theoretical and numerical estimates of M_2 tidal conversion over a steep oceanic ridge to develop confidence in both approaches. The analytical estimates of tidal conversion rate (St. Laurent et al. 2003; Llewellyn Smith and Young 2002; Pétrélis et al. 2006) are obtained by ignoring diffusion, viscosity, and nonlinearity. With this neglect, the solutions in the supercritical regime are singular. This singularity of the linear and inviscid solution indicates missing physics and leads one to wonder if the resulting theoretical estimates of tidal conversion are compromised. However, comparisons with numerical estimates of tidal conversion obtained with a nonlinear primitive equation ocean model reveal very good agreement between theory and model (Figs. 2 and 3). The model

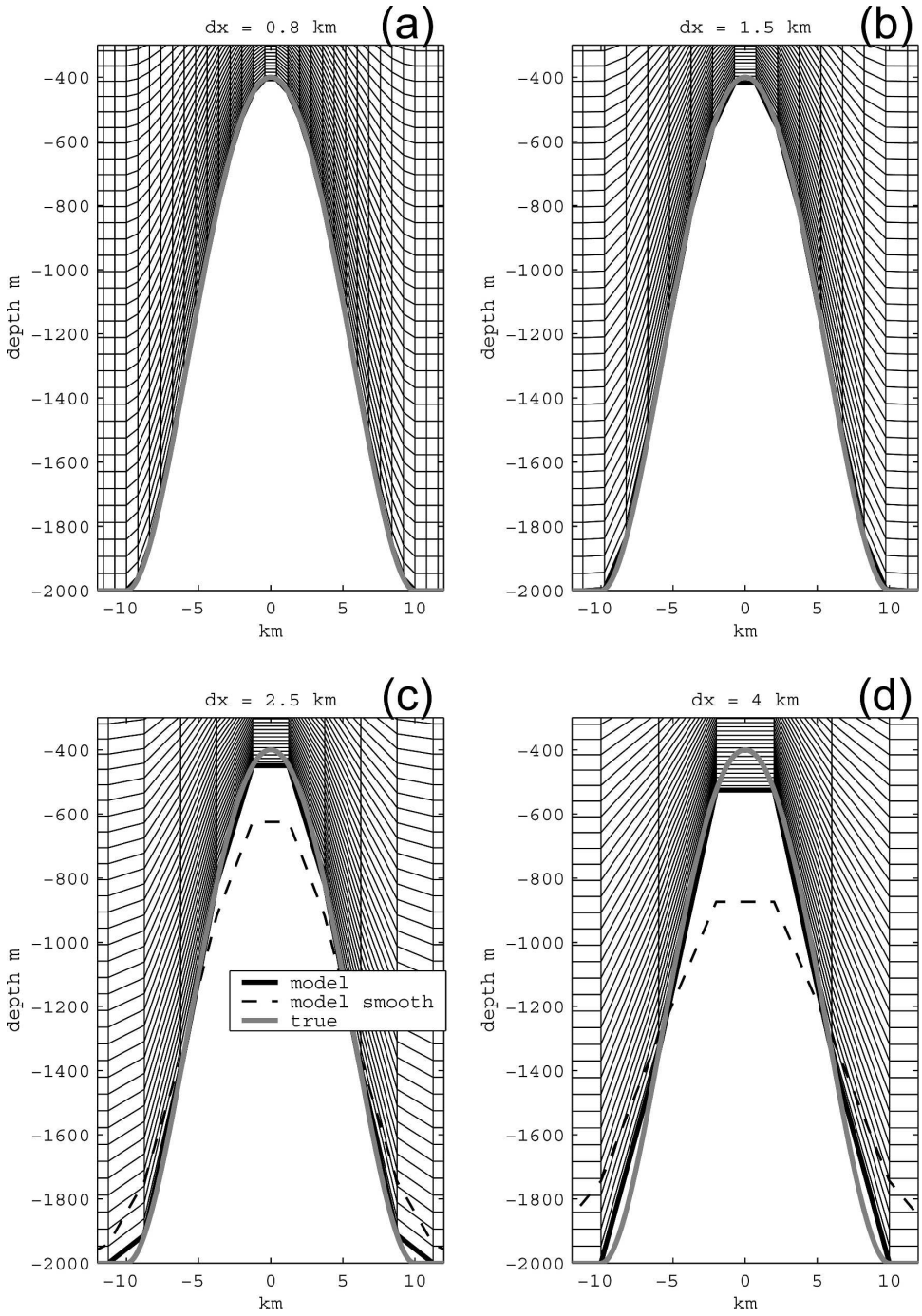

FIG. 5. Model grid representation of the polynomial ridge using different horizontal resolutions, *dx*: (a) 0.8, (b) 1.5, (c) 2.5, and (d) 4 km. The thick gray line is the analytic function for the ridge. The thick black line is the model representation with no smoothing; the dashed thick line is after the smoothing. A Shapiro filter is used for the smoothing (see text for more details).

predicts on average a 2.5% lower conversion rate than theory (with a standard error deviation of 3.5%). Because of its finite resolution the model smooths the singularities along the tidal beams. In other words, the model will only represent the first few vertical modes accurately, therefore leading to an underestimate of tidal conversion when compared with the analytical prediction. Figure 7 shows the perturbation velocity fields and the isopycnals associated with the internal waves for different heights of the ridge. As the height of

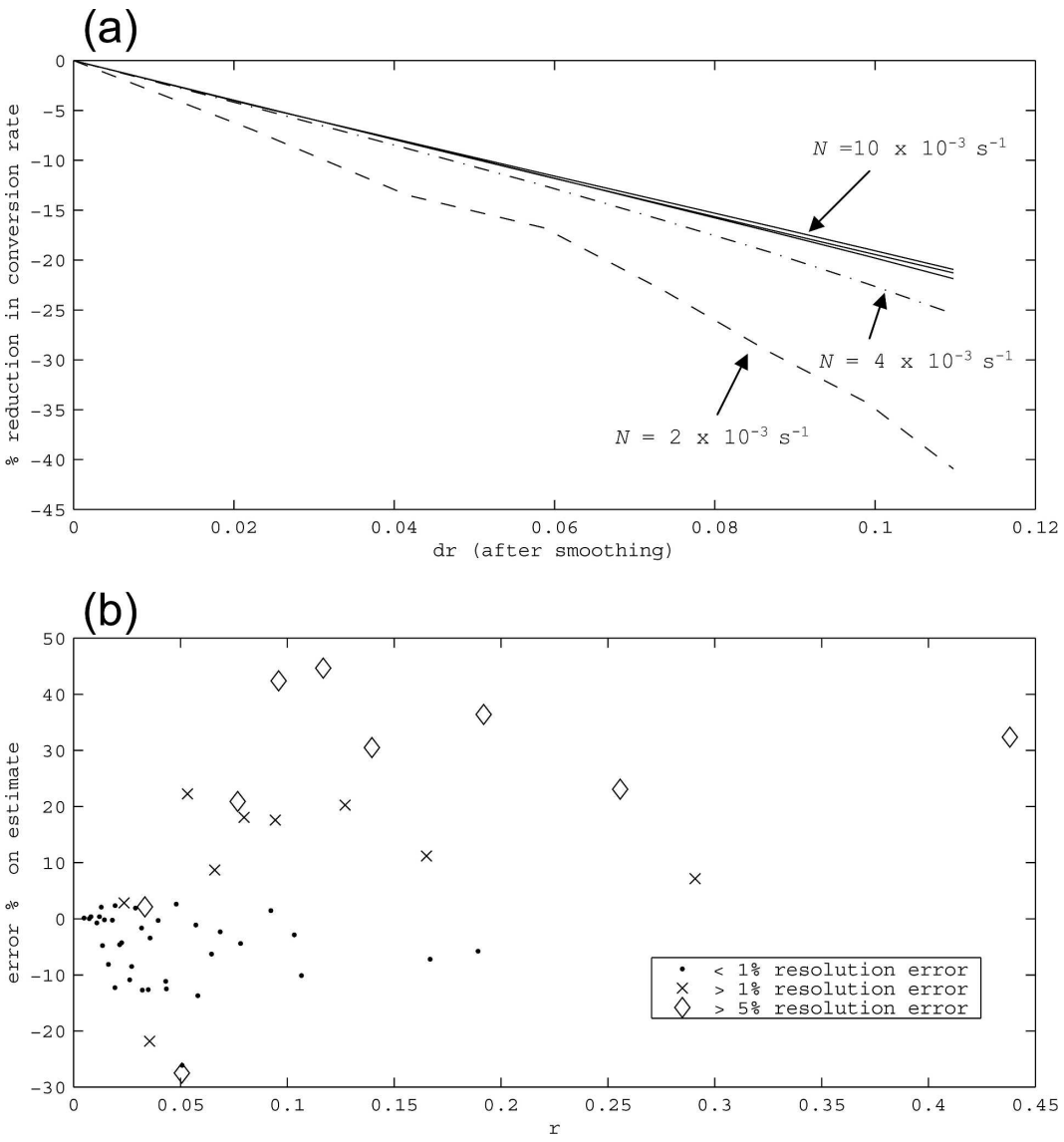

FIG. 6. (a) Percent reduction in tidal conversion due to smoothing of the ridge. The amount of smoothing is indicated on the x axis as the change (dr) in the r factor, which is an indication of the topographic slope. The different lines are for different values of N. (b) Percent error deviation of model tidal conversion estimates from the analytical prediction as a function of the r factor. The different symbols denote different levels of errors in spatially resolving the ridge (see text in section 4 for definition).

the ridge increases, we make a transition toward more supercritical regimes and the slope of the isopycnals becomes much steeper in proximity of the ridge. This is consistent with the theoretical limit of a singularity along the beams. Within 200 km of the ridge, dissipation in the model acts in reducing the slope of the isopycnals with a loss of about 30% of the converted initial energy (Fig. 4). A sensitivity analysis reveals that the model predictions are insensitive to vertical viscosity/diffusivity in the range from 0 to 10^{-3} m^2 s^{-1}, suggesting that the numerical dissipation associated with the differencing scheme is already sufficient to remove the singularity in the solutions. To see significant reduction of the conversion rate we needed to increase the explicit viscosity/diffusivity up to 10^{-1} m^2 s^{-1}.

These results are a successful mutual validation of numerical models and analytical theory in quantifying the conversion from barotropic to baroclinic tidal energy. However, they also reveal some of the limitations associated with both approaches. Analytical estimates are useful, as they provide the tidal conversion rate over the ridge, but are unable to predict the decay of

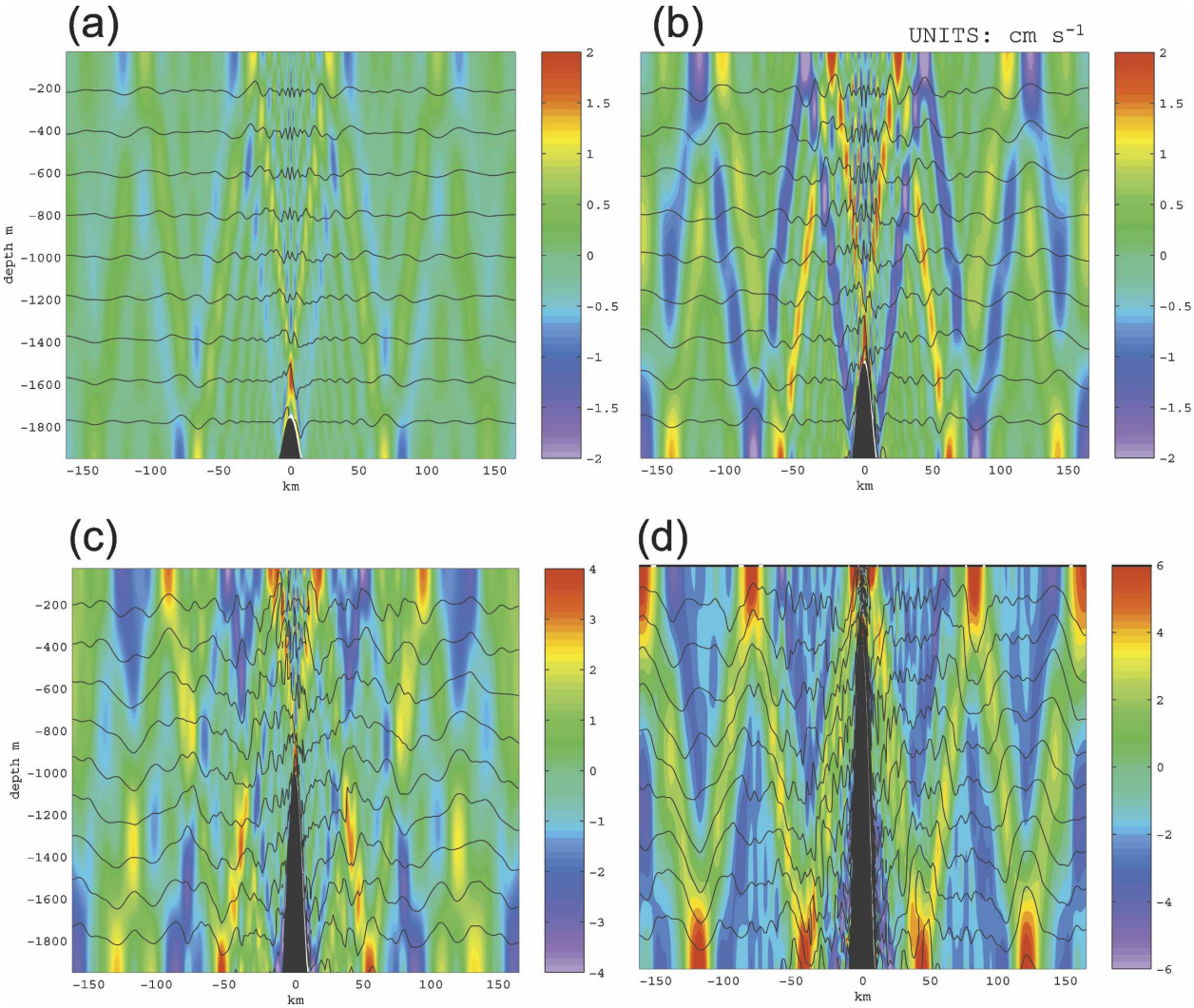

FIG. 7. Vertical sections of baroclinic U velocities (cm s^{-1}) associated with the internal wave field for different heights of the bump: (a) 240 m, subcritical; (b) 500 m, transitional regime; and (c) 1000 and (d) 1600 m, supercritical regime. The isopycnals (black lines) are increased in magnitude by a factor of 10 to show the perturbations associated with the internal tides. The maximum barotropic tidal velocity amplitude is 2 cm s^{-1}, and the total extent of the domain in the x direction is ± 600 km.

energy flux occurring beyond 50–200 km from the ridge. Over this distance the model predicts a significant reduction in the wave energy flux associated with dissipation (30%). However, it is unclear if these dissipative effects are representative of the actual physical processes or an artifact of numerical dissipation. We cannot distinguish in the model between numerical and explicit dissipation in the range of viscosity/diffusivity typical of the ocean. Although observations (Klymak et al. 2006; Rudnick et al. 2003) are consistent with the idea that a large fraction (20%–30%) of the converted energy is dissipated within a few hundred kilometers from the ridge, the physical processes responsible for this (e.g., nonhydrostatic effects) are clearly not resolved and are crudely represented in the model.

As a result of the numerical simulations we also show that the conversion estimates are sensitive to the correct representation of the topographic features. For example, small amounts of topographic smoothing needed to run s-coordinate general circulation ocean models may lead to significant underestimates of the tidal conversion. In section 4c we show that after smoothing the topography and reducing the topographic slope, relative to the model grid, by 0.1 (the r factor) we obtain an underestimate of tidal conversion of about 20%. This ratio of smoothing over reduction of tidal conversion is found to be robust for the stratification range observed in the ocean ($N = 10^{-3}$ to 10^{-2} s^{-1}). As a provocative exercise we took the Sandwell and Smith (1997) topography at 3.5-km resolution over

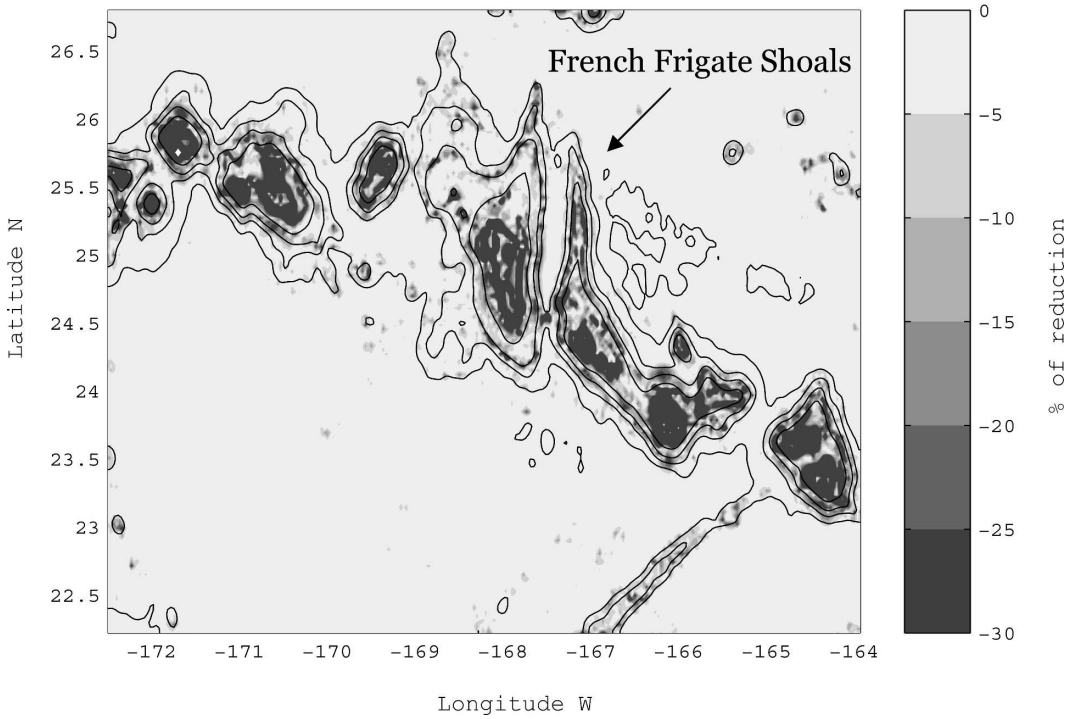

FIG. 8. Estimate of the percent reduction in tidal conversion as a result of smoothing the topography in a section of the Hawaiian Ridge. The smoothing is often required to run ocean models that do not fully resolve the topographic slopes (see text for details). Estimates are derived using the results from section 4 obtained by smoothing analytical ridge shapes.

a portion of the Hawaiian Ridge, which in places has an r factor as large as 0.9 and is consistently greater than 0.2 in proximity of the steep portions of the ridge, and smoothed it to keep the r factor below 0.2 (see section 4c for definition). This is a common requirement in modeling studies that use a stretched vertical coordinate system in order to reduce the error deriving from the computation of the pressure gradient term (Mellor et al. 1994) in the horizontal momentum equations. The smoothing applied was a Shapiro filter and water depths below 50 m were set to 50 m. We then used the results from Fig. 6a to estimate the reduction in tidal conversion (Fig. 8: the color axes are set from 0% to −30%, although there are values below –50% in the proximity of the maximum elevation of the ridge). The results show that in the proximity of the ridge one should expect an underestimate of more than 30%. However, this percentage is very sensitive to the type of filter used to smooth the topography and the resolution of the model grid. In general one can test the effect of the filter by using the analytical prediction for the polynomial ridge before and after the smoothing. We also find that not smoothing the topography and not having adequate horizontal resolution can lead to significant overestimates (e.g., by 35%). We therefore suggest that topographic misrepresentation error is an important component of the tidal conversion problem, and it may explain some of the discrepancies in current numerical estimates of conversion and internal tides energy flux over realistic oceanic regions.

Acknowledgments. This research was partially funded by NASA Goddard Grant NAG5-12388. We thank Gary Egbert for useful comments and Alexander Shchepetkin for advice on the numerical calculations.

APPENDIX

Computation of the Wave Energy Flux in the Regional Ocean Modeling System Using Sigma Coordinates

The energy flux [Eq. (1)] in sigma coordinates is proportional to

$$Ef(x,t) \approx \int_{-1}^{0} p'(x,s,t)u'(x,s,t)H_z\, ds, \quad H_z \equiv \frac{\partial z}{\partial s},$$

where H_z is the thickness in units of length of the sigma layer. We have omitted the remaining terms and integrals that do not need to be transformed in sigma co-

ordinate. The computation of $u'(x, s, t)$ is straightforward, as the model already provides the vertical integral u_B:

$$u'(x, s, t) = u(x, s, t) - u_B(s, t).$$

To evaluate $p'(x, s, t)$ we use the same numerical scheme used in ROMS to compute the pressure. The input arguments to compute pressure are

$$\mathrm{PRS} = \mathrm{PRS}[\rho, z(s, \eta, t)].$$

We first define the total pressure without the contribution of the free surface and the pressure of the state of rest as follows:

$$p_T(s, t) = \mathrm{PRS}[\rho(s, t), z(s, 0, 0)] \quad \text{and}$$

$$p_0(s, 0) = \mathrm{PRS}[\bar{\rho}(s), z(s, 0, 0)].$$

We now define the baroclinic pressure p' associated with the internal waves as

$$p_I = p_T - p_0 \quad \text{and}$$

$$p'(s, t) = p_I - \int_{-1}^{0} p_I H_z \, ds.$$

Note that, by subtracting the integral of p_I, this definition of p' does not include the contribution from the free surface, for example, the term $\rho_0 g(\eta - \eta_B)$ that appears in the definition of perturbation pressure in section 2c. This term is omitted because it vanishes in the computation of the energy flux.

REFERENCES

Althaus, A. M., E. Kunze, and T. B. Sanford, 2003: Internal tide radiation from Mendocino Escarpment. *J. Phys. Oceanogr.,* **33,** 1510–1527.

Balmforth, N. J., G. R. Ierley, and W. R. Young, 2002: Tidal conversion by subcritical topography. *J. Phys. Oceanogr.,* **32,** 2900–2914.

Bell, T. H., 1975: Topographically generated internal waves in the open ocean. *J. Geophys. Res.,* **80,** 320–327.

Cummins, P. F., J. Y. Cherniawsky, and M. G. G. Foreman, 2001: North Pacific internal tides from the Aleutian Ridge: Altimeter observations and modeling. *J. Mar. Res.,* **59,** 167–191.

Egbert, G. D., and R. D. Ray, 2000: Significant dissipation of tidal energy in the deep ocean inferred from satellite altimeter data. *Nature,* **405,** 775–778.

——, and ——, 2001: Estimates of *M*-2 tidal energy dissipation from TOPEX/Poseidon altimeter data. *J. Geophys. Res.,* **106,** 22 475–22 502.

Garrett, C., and L. St. Laurent, 2002: Aspects of deep ocean mixing. *J. Oceanogr.,* **58,** 11–24.

Haidvogel, D. B., and A. Beckmann, 1999: *Numerical Ocean Circulation Modeling.* Imperial College Press, 312 pp.

——, H. G. Arango, K. Hedstrom, A. Beckmann, P. Malanotte-Rizzoli, and A. F. Shchepetkin, 2000: Model evaluation experiments in the North Atlantic Basin: Simulations in nonlinear terrain-following coordinates. *Dyn. Atmos. Oceans,* **32,** 239–281.

Kang, S. K., M. G. G. Foreman, W. R. Crawford, and J. Y. Cherniawsky, 2000: Numerical modeling of internal tide generation along the Hawaiian Ridge. *J. Phys. Oceanogr.,* **30,** 1083–1098.

Khatiwala, S., 2003: Generation of internal tides in an ocean of finite depth: Analytical and numerical calculations. *Deep-Sea Res. I,* **50,** 3–21.

Klymak, J. M., and Coauthors, 2006: An estimate of tidal energy lost to turbulence at the Hawaiian Ridge. *J. Phys. Oceanogr.,* **36,** 1148–1164.

Llewellyn Smith, S. G. L., and W. R. Young, 2002: Conversion of the barotropic tide. *J. Phys. Oceanogr.,* **32,** 1554–1566.

——, and ——, 2003: Tidal conversion at a very steep ridge. *J. Fluid Mech.,* **495,** 175–191.

Marchesiello, P., J. C. McWilliams, and A. Shchepetkin, 2003: Equilibrium structure and dynamics of the California Current system. *J. Phys. Oceanogr.,* **33,** 753–783.

Mellor, G. L., T. Ezer, and L. Y. Oey, 1994: The pressure gradient conundrum of sigma coordinate ocean models. *J. Atmos. Oceanic Technol.,* **11,** 1126–1134.

Merrifield, M. A., and P. E. Holloway, 2002: Model estimates of M_2 internal tide energetics at the Hawaiian Ridge. *J. Geophys. Res.,* **107,** 3179, doi:10.1029/2001JC000996.

Munk, W., and C. Wunsch, 1998: Abyssal recipes II: Energetics of tidal and wind mixing. *Deep-Sea Res. I,* **45,** 1977–2010.

Niwa, Y., and T. Hibiya, 2001: Numerical study of the spatial distribution of the *M*-2 internal tide in the Pacific Ocean. *J. Geophys. Res.,* **106,** 22 441–22 449.

Pétrélis, F., S. G. Llewellyn Smith, and W. R. Young, 2006: Tidal conversion at a submarine ridge. *J. Phys. Oceanogr.,* **36,** 1053–1071.

Polzin, K., 2004: Idealized solutions for the energy balance of the finescale internal wave field. *J. Phys. Oceanogr.,* **34,** 231–246.

Robinson, R. M., 1969: The effects of a barrier on internal waves. *Deep-Sea Res.,* **16,** 412–429.

Rudnick, D. L., and Coauthors, 2003: From tides to mixing along the Hawaiian Ridge. *Science,* **301,** 355–357.

Sandwell, D. T., and W. H. F. Smith, 1997: Marine gravity anomaly from *Geosat* and *ERS 1* satellite altimetry. *J. Geophys. Res.,* **102,** 10 039–10 054.

Shchepetkin, A. F., and J. C. McWilliams, 1998: Quasi-monotone advection schemes based on explicit locally adaptive dissipation. *Mon. Wea. Rev.,* **126,** 1541–1580.

——, and ——, 2003: A method for computing horizontal pressure-gradient force in an oceanic model with a nonaligned vertical coordinate. *J. Geophys. Res.,* **108,** 3090, doi: 10.1029/2001JC001047.

St. Laurent, L., S. Stringer, C. Garrett, and D. Perrault-Joncas, 2003: The generation of internal tides at abrupt topography. *Deep-Sea Res. I,* **50,** 987–1003.